Available online at www.sciencedirect.com
SCIENCE DIRECT®
Inorganica Chimica Acta 359 (2006) 391–400
Inorganica Chimica Acta
www.elsevier.com/locate/ica

Synthesis, characterization and structure of ruthenium(II) phosphine complexes with N-heterocyclic thiolate ligands

Solange O. Pinheiro [a], Jackson R. de Sousa [a], Marcelo O. Santiago [a], Idalina M.M. Carvalho [a], Ana L.R. Silva [a], Alzir A. Batista [b], Eduardo E. Castellano [c], Javier Ellena [c], Ícaro S. Moreira [a], Izaura C.N. Diógenes [a,*]

[a] *Departamento de Química Orgânica e Inorgânica, Universidade Federal do Ceará, Cx Postal 12200, 60455-760 Fortaleza, CE, Brazil*
[b] *Departamento de Química, Universidade Federal de São Carlos, Cx Postal 676, 13565-905 São Carlos, SP, Brazil*
[c] *Instituto de Física de São Carlos, Universidade de São Paulo, Cx Postal 780, 13560-250 São Carlos, SP, Brazil*

Received 21 December 2004; received in revised form 11 April 2005; accepted 5 May 2005
Available online 20 December 2005

Abstract

The [Ru(dppb)(mbt)$_2$], mbt = 2-mercaptobenzothiazole, complex, isolated from the reaction of the *mer*-[RuCl$_3$(dppb)(OH$_2$)] complex with the 2,2′-dithiobis(benzothiazole), mbts, was characterized by spectroscopic and electrochemical techniques ($E_{1/2} = 0.78$ V versus NHE) and its structure was determined by crystal X-ray analysis. The structural analysis suggests that the S–S bond of the mbts ligand is cleaved, thus forming two four-membered chelate rings coordinated to the ruthenium through the N,S-donor atoms of the mbt reduced ligands, with an average bite angle of 67.295(11)°. The ^{1}H and ^{13}C NMR signals observed for mbts ligand coordinated to the metal center, the changes in the vibrational spectra, and the appearance of a MLCT band in the electronic spectrum of the complex point for the reduced state of the ruthenium metal center, Ru^{II}. These reducing processes are suggested to be due to the methanol interference, which is observed to be strongly affected by *N*-methylmorpholine. The cytochrome *c* electrochemistry was analyzed by using the SAMs formed by the mbts and the [Ru(dppb)(mbt)$_2$] complex on gold, with only the former presenting electroactivity.

Keywords: Ruthenium phosphine compounds, N-Heterocyclic thiolate ligands; Chemically modified electrode; SAM; SERS; Cyt *c*

1. Introduction

The π-back-bonding capability of the Ru(II) complexes together with the singular properties of phosphine ligands [1] constitute interesting aspects concerning the possibility of make thin inorganic films with potential coordination chemistry on surface [2]. Many studies have focused on altering the physical-chemistry properties of these materials by introducing different substituents or metal centers with different backbone capacities. This allows tuning of the electronic properties which may have applications in electrocatalysis or chemical sensing involving the pendant moieties of a given complex.

Self-assembled monolayers (SAMs) formed by organothiol species, which are ordered and highly packed, are usually used as sensors in a general sense. For instance, the redox process of cytochrome *c* (cyt *c*) metalloprotein has been electrochemically studied [3–5] by using gold electrode modified by the organothiol ligand 4-mercaptopyridine (pyS). In a series of paper [6–8], it has been demonstrated that the π-back-bonding interaction capability of the $[M^{II}(CN)_5]^{3-}$ (M = Fe and Ru) metal center enhances the interaction between the gold atoms and the pyS sulfur head group portion. Another example that may be reported here is the direct electrochemistry of folic acid at a 2-mercaptobenzothiazole (mbt) SAM on gold

* Corresponding author. Tel.: +55 0318532889844; fax: +55 03185328 89978.
E-mail address: izaura@dqoi.ufc.br (I.C.N. Diógenes).

0020-1693/$ - see front matter © 2005 Elsevier B.V. All rights reserved.
doi:10.1016/j.ica.2005.05.042

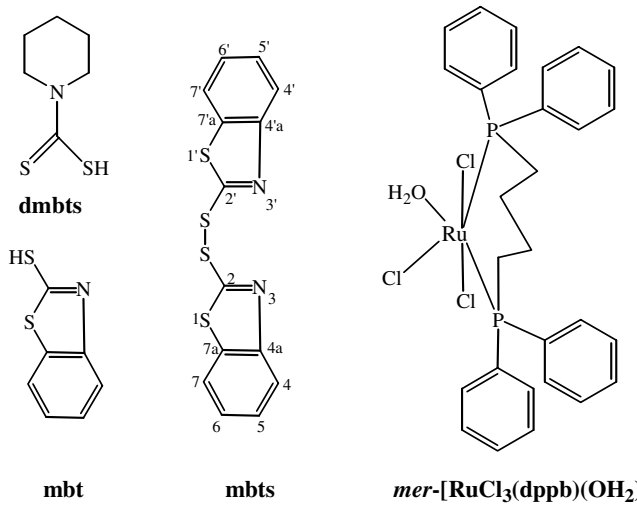

Chart 1. Planar representations of the dmbts, mbt, mbts ligands and the *mer*-[$RuCl_3$(dppb)(OH_2)] complex.

electrode (mbt/SAM/Au) [9]. The good performance of this SAM in determining folic acid in solution was assigned to the mbt ability in strongly binding to gold forming a closely packed monolayer that enhances the inherent electron transfer rate equilibrium constant.

Aiming to evaluate the electronic properties of the metal center upon the attachment of a conjugated substituent and develop a system with a potential application to act as a mimetic biosensor and to be used in the catalysis field, we have been characterizing and studying the properties of the compound isolated from the reaction of the 2,2′-dithiobis(benzothiazole) (mbts) ligand with the *mer*-[$Ru^{III}Cl_3$(dppb)(OH_2)] complex, where dppb = 1, 4-bis(diphenylphosphine)butane. For correlation purposes, the complex isolated from the reaction of [$Ru^{II}Cl_2$(dppb)-(PPh_3)] with the piperidinedithiocarbamate (dmbts) ligand was also characterized. The planar representations of these compounds are illustrated in Chart 1.

2. Experimental

2.1. Materials

The water used throughout was purified by a Milli-Q system (Millipore Co.). The *mer*-[$RuCl_3$(dppb)(OH_2)] and [$RuCl_2$(dppb)(PPh_3)] complexes were synthesized according to the literature [10,11]. Sodium piperidinedithiocarbamate, $C_6H_{10}S_2NNa$ (dmbts), was synthesized according to the method reported in the literature [12]. The 2,2′-dithiobis(benzothiazole) organothiol ligand, potassium hydroxide, potassium phosphate (KH_2PO_4) and *N*-methylmorpholine (Aldrich) were used without previous purification. Hexane, ethanol, diethyl ether and methanol solvents were purchased from Merck and used as received. Dichloromethane of HPLC grade (Merck) was treated by refluxing over CaH_2 and distilled twice before its electrochemical usage. Tetrabutylammonium perchlorate (TBAP), from Fluka, was recrystallized twice from absolute ethanol and dried under vacuum. The Suprapur H_2SO_4 (Merck) was used as received. Horse heart cytochrome *c* (type VI, 99%, Aldrich Co.) was purified as described in the literature [13].

The [Ru(dppb)($mbt)_2$] complex was isolated from the reaction of *mer*-[$RuCl_3$(dppb)(OH_2)] with the mbts ligand following the procedure described in the literature for similar complexes [10,14]. A 29.99 mg sample (0.046 mmol) of the *mer*-[$RuCl_3$(dppb)(OH_2)] complex was dissolved in 2 mL of methanol, under argon atmosphere. In another flask, an equimolar quantity of the mbts ligand was dissolved in CH_2Cl_2, in anaerobic conditions. After total dissolution of both reagents, the *mer*-[$RuCl_3$(dppb)-(OH_2)] complex solution was slowly transferred to the flask containing the ligand and a few drops (160 μL) of *N*-methylmorpholine was added. This last compound was used to confer a basic medium reaction aiming to facilitate the mbts coordination to the metal center. The resulting solution developed a pale green color and was allowed to stand for 4 h in the absence of light, under stirring and argon flow. The green precipitate formed during the reaction was collected by filtration, washed with hexane, dried, and stored under vacuum in the absence of light. Yield: 86%. *Anal*. Calc. for [Ru(dppb)($mbt)_2$]: C, 26.09; H, 2.63, N, 18.27. Found: C, 26.31; H, 2.59; N, 18.58%.

The [Ru(dppb)($dmbts)_2$] compound was obtained from the reaction of the [$RuCl_2$(dppb)(PPh_3)] complex with the dmbts ligand. A 40.32 mg sample (0.25 mmol) of this ligand was added to a solution of CH_2Cl_2/CH_3OH (80/20) containing 86.07 mg (0.10 mmol) of the [$RuCl_2$(dppb)-(PPh_3)] complex. The reaction was allowed to proceed for 3 h, under stirring and argon flow, at room temperature. The resulting yellow solution was concentrated to near 1 mL volume followed by the addition of 10 mL of diethyl ether. The yellow precipitate formed was collected, washed with diethyl ether, and dried under vacuum in the absence of light. Yield: 86%. *Anal*. Calc. for [Ru(dppb)($dmbts)_2$]: C, 56.65; H, 5.70; N, 3.30. Found: C, 57.30; H, 5.80; N, 3.35%.

The electrochemical data obtained for the cyt *c* with gold electrodes modified with the [Ru(dppb)($mbt)_2$] complex and mbts ligand were correlated with those acquired with the gold surface modified with the $[Ru(CN)_5(pyS)]^{4-}$ complex [7], where pyS = 4-mercaptopyridine. Because of this, the $[Ru(CN)_5(pyS)]^{4-}$ complex was synthesized according to the literature procedures [7].

2.2. Apparatus

Crystallographic data were performed with graphite monochromated Mo Kα ($\lambda = 0.71073$ Å) radiation on an Enraf-Nonius Kappa-CCD diffractometer. Data were collected up to 50° in 2θ, with a redundancy of 4. The final unit cell parameters were based on all reflections. Data collections were made using the COLLECT program

[15]; integration and scaling of the reflections were performed with the HKL Denzo-Scalepack system of programs [16]. Absorption corrections were carried out using the multi-scan method [17]. The structures were solved by direct methods with SHELXS-97 [18]. The model was refined by full-matrix least-squares on F^2 by means of SHELXL-97 [18]. All the hydrogen atoms were located on stereochemical grounds, stereochemically positioned and refined with the riding model [19]. The data collections and experimental details for the complexes are summarized in Table 1.

The electronic spectra of the complexes and ligands were acquired with a *Hitachi* model *U*-2000 spectrophotometer. The transmission infrared spectra of the compounds dispersed in KBr were obtained by using a *Perkin–Elmer* instrument model *Spectrum 1000*. ^{1}H and ^{13}C NMR normal and two-dimension COSY ^{1}H–^{1}H and HMQC ^{1}H–^{13}C spectra were recorded on Bruker AVANCE 500 spectrometer and referenced to the residual proton solvent resonances ($CDCl_3$, δ 7.27). ^{31}P{^{1}H} NMR spectra were obtained on a T BRUKER DRX400 spectrometer at 298K, using H_3PO_4 85% as external reference for ^{31}P{^{1}H} (161 MHz). Electrochemical experiments were performed with an electrochemical analyzer BAS *100W* from Bioanalytical System at 25 ± 0.2°C. TBAP was used as supporting electrolyte for all electrochemical measurements performed in nonaqueous medium. For these experiments, a reference Ag/AgCl electrode, prepared only at the working day for about 1 h before the experiments beginning, was used as reference electrode. The potentials reported in this study, however, were all converted to the normal hydrogen electrode (NHE), based on the ferrocene/ferrocenium ($Fc^{+/0}$) redox process, which was observed at 0.64 V in CH_2Cl_2. A conventional three-electrode glass cell with a platinum disk (0.0314 cm^2 of geometrical area) and foil as working and auxiliary electrodes, respectively, was used for the complexes and ligand characterizations.

The electrochemical experiments with cyt *c* were carried out by using a three-electrode configuration cell where the working electrode was polycrystalline gold surface modified with the mbts ligand, and with $[Ru(CN)_5(pyS)]^{4-}$ and $[Ru(dppb)(mbt)_2]$ complexes. The 0.1 M phosphate (KH_2PO_4) buffer aqueous solution, pH 7.0, was used as electrolyte, at room temperature. Before the experiments, the cyt *c* solutions were stored at 4 °C in order to avoid protein denaturizing process [20]. A BAS Ag|AgCl|Cl (3.5 M KCl) and a gold flag were used as reference and auxiliary electrodes, respectively. The surface modification procedure was made by immersing the gold electrodes in a saturated aqueous solution of the ligand or the complex for at least 2 h. For comparative purpose, the modification of a gold surface with the $[Ru(CN)_5(pyS)]^{4-}$ complex (RupySAu) was also performed by immersing the electrode in a 20 mM complex aqueous solution for 15 min as reported in the literature [7].

The ex situ surface enhanced Raman scattering (SERS) spectra of the SAMs were acquired by using a *Renishaw Raman Imaging Microscope System 3000* equipped with a charge coupled device (CCD) detector, and an Olympus (BTH2) with 50× objective to focus the laser beam on the sample in a backscattering configuration. As exciting radiation, λ_0, the 632.8 nm line from a He–Ne (*Spectra-Physics*) laser was used. The gold substrates used for spectra SERS acquisition were activated by the oxidation–reduction cycles (ORC) procedure in 0.1 M KCl as described by Gao et al. [21], without the active species in solution. The activation of the gold surface for SERS spectra acquisition was made by using a PAR 273 potentiostat.

The polishing procedure of the gold surfaces employed in different experiments cited above was made as described by Qu et al. [22]. These electrodes were mechanically polished with alumina paste of different grades to a mirror finish, rinsed and sonicated (10 min) with Milli-Q water. Then, the electrode was immersed in a freshly prepared "piranha solution" (3:1 concentrated H_2SO_4/30% H_2O_2 – *Caution*: the "piranha solution" is a strong oxidant solution that reacts violently with organic compounds), rinsed exhaustively with water and sonicated again. The cleanness was evaluated by comparison of the *i* versus *E* curve obtained in a 0.5 M H_2SO_4 solution with the well-established curve for a clean gold surface [23].

Table 1
Crystallographic data and structure refinement for $[Ru(dppb)(mbt)_2]$ and $[Ru(dppb)(dmbts)_2]$ complexes

Compound	$[Ru(dppb)(mbt)_2]$	$[Ru(dppb)(dmbts)_2]$
Empirical formula	$[C_{42}H_{36}N_2P_2S_4Ru]$ · $CH_3CH_2OCH_2CH_3$	$[C_{40}H_{48}N_2P_2S_4Ru]$ · CH_2Cl_2
Formula weight	934.10	932.98
Temperature (K)	293(2)	120(2)
Crystal system	triclinic	triclinic
Crystal size (mm^3)	0.08 × 0.06 × 0.04	0.12 × 0.06 × 0.04
Space group	$P\bar{1}$	$P\bar{1}$
Unit cell dimensions		
a (Å)	11.3178(9)	2.1946(4)
b (Å)	12.849(1)	12.5932(5)
c (Å)	16.508(1)	15.1898(7)
α (°)	104.652(6)	95.887(2)
β (°)	107.832(5)	108.169(2)
γ (°)	92.206(5)	104.120(2)
V ($Å^3$)	2193.4(3)	2108.6(2)
Z	2	2
D_{calc} (Mg/m^3)	1.414	1.469
Absorption coefficient (mm^{-1})	0.658	0.805
F(000)	964	964
θ Range for data collection (°)	2.93–25.00°	2.43–25.00°
Reflections collected	13 570	13 762
Independent reflections (R_{int})	7712 (0.0662)	7372 (0.0818)
Final *R* indices [$I > 2\sigma(I)$]	$R_1 = 0.0541$, $wR_2 = 0.0989$	$R_1 = 0.0575$, $wR_2 = 0.1505$
R indices (all data)	$R_1 = 0.1214$, $wR_2 = 0.1189$	$R_1 = 0.0849$, $wR_2 = 0.1656$

3. Results and discussion

3.1. Crystal and molecular structure

Recrystallization of the [Ru(dppb)(mbt)$_2$] and [Ru(dppb)(dmbts)$_2$] complexes from dichloromethane/diethyl ether solutions yielded pale green and yellow crystals, respectively, suitable for single crystal X-ray analyses. Both complexes crystallize in the $P\bar{1}$ triclinic space group with the ruthenium environments adopting a distorted octahedral geometry in which the nitrogen and sulfur atoms, respectively, are *trans* to the phosphorous atoms. Selected bond lengths (Å) and angles (°) are displayed in Table 2 for these crystals.

The ORTEP views of the structures are shown in Fig. 1. The molecular structure for the [Ru(dppb)(mbt)$_2$] complex, Fig. 1A, reveals two units of the 2-mercaptobenzothiazole ligand coordinated to the ruthenium metal center as a bidentate N,S-donor, forming two four-membered chelate ring with an average bite angle of 67.295(11)°. It is clear from the structure illustrated in Fig. 1A that for each mbt ligand bonded to ruthenium, there is a non-coordinated sulfur atom in the ring and only one sulfur atom coordinated to the metal center. This suggests that upon coordination to ruthenium, the S–S bond is broken through reduction of the mbts ligand. For the [Ru(dppb)(dmbts)$_2$] complex, the X-ray analysis points also for a structure with bidentate S,S-donor covalently bonded to the ruthenium metal center (Fig. 1B), with an average bite angle of 71.515(4)°.

Table 2
Selected bond lengths (Å) and angles (°) for [Ru(dppb)(mbt)$_2$], [Ru(dppb)(dmbts)$_2$] and complexes with estimated deviations in parentheses

Bond length (Å)			
[Ru(dppb)(mbt)$_2$]		[Ru(dppb)(dmbts)$_2$]	
Ru–N(1)	2.143(4)	Ru–S(12)	2.4407(13)
Ru–N(2)	2.167(4)	Ru–S(22)	2.4497(12)
Ru–P(1)	2.2697(15)	Ru–P(1)	2.2837(13)
Ru–P(2)	2.2733(14)	Ru–P(2)	2.2959(12)
Ru–S(11)	2.4430(14)	Ru–S(11)	2.4101(13)
Ru–S(21)	2.4559(14)	Ru–S(21)	2.4136(13)
Bond angle (°)			
RudppbMBTS		RudppbDMBTS	
N(1)–Ru–N(2)	82.20(15)	S(21)–Ru–S(22)	71.54(4)
N(1)–Ru–P(1)	91.06(11)	S(11)–Ru–S(22)	95.28(4)
N(2)–Ru–P(1)	171.48(11)	S(11)–Ru–S(12)	71.49(4)
N(1)–Ru–P(2)	166.14(11)	S(21)–Ru–S(12)	88.46(4)
N(2)–Ru–P(2)	92.49(11)	P(1)–Ru–S(22)	87.21(4)
P(1)–Ru–P(2)	95.23(6)	P(1)–Ru–S(11)	102.18(5)
N(1)–Ru–S(11)	67.69(11)	P(1)–Ru–S(12)	170.08(4)
N(2)–Ru–S(11)	94.53(11)	P(1)–Ru–S(21)	96.03(5)
P(1)–Ru–S(11)	87.67(5)	P(1)–Ru–P(2)	94.28(5)
P(2)–Ru–S(11)	100.18(5)	P(2)–Ru–S(22)	176.30(4)
N(1)–Ru–S(21)	96.64(11)	P(2)–Ru–S(12)	93.10(4)
N(2)–Ru–S(21)	66.90(11)	P(2)–Ru–S(21)	104.91(4)
P(1)–Ru–S(21)	108.99(5)	P(2)–Ru–S(11)	87.73(4)
P(2)–Ru–S(21)	92.98(5)	S(12)–Ru–S(22)	85.83(4)
S(11)–Ru–S(21)	157.80(5)	S(11)–Ru–S(21)	157.02(5)

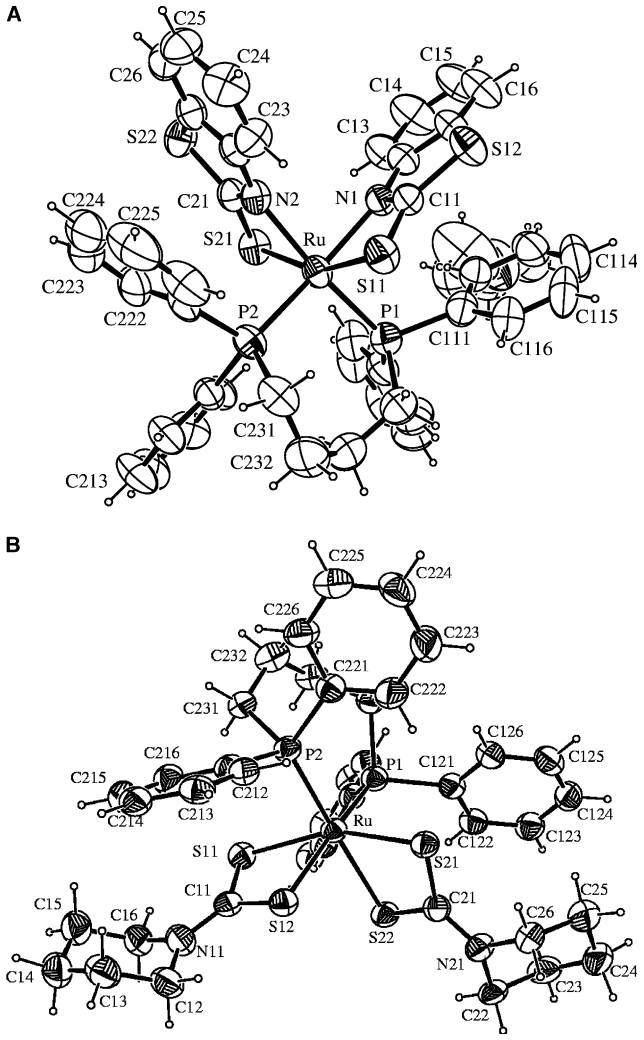

Fig. 1. ORTEP [19] diagrams for the asymmetric units of (A) [Ru(dppb)(mbt)$_2$] and (B) [Ru(dppb)(dmbts)$_2$] complexes, showing the atoms labelling and the 50% probability ellipsoids.

As no other reducing agent was inserted in the reactional medium, the reducing of the S–S bridge of the mbts ligand, as well as the redox process of the ruthenium metal center ($Ru^{III} \rightarrow Ru^{II}$), is proposed to be due to the methanol interference. In fact, the literature report for some synthetic methods of ruthenium complexes, that the reduction of Ru(III) to Ru(II) occurs by organic solvents [24]. An interesting experimental observation that must be addressed here is the fact that the synthesis of the [Ru(dppb)(mbt)$_2$] complex is strongly facilitated in the presence of *N*-methylmorpholine. Similar procedure was made with no *N*-methylmorpholine in solution and the compound isolated was found to be not pure and completely different.

The deviation from the ideal octahedral geometry can be seen by the angles between P(1)–Ru–P(2) 95.23(6)°, N(2)–Ru–S(21) 66.90(11)°; N(1)–Ru–S(11) 67.69(11)° for the [Ru(dppb)(mbt)$_2$] complex and P(1)–Ru–P(2) 94.28(5)°; S(11)–Ru–S(12) 71.49(4)°; S(21)–Ru–S(22) 71.54(4)° for the [Ru(dppb)(dmbts)$_2$] complex. Attention must be paid

for the N–Ru–S and S–Ru–S angles of $[Ru(dppb)(mbt)_2]$ and $[Ru(dppb)(dmbts)_2]$ complexes, respectively. Almost sure, the geometrical arrangement of the mbt or dmbts moieties in the $[Ru(dppb)(mbt)_2]$ or $[Ru(dppb)(dmbts)_2]$ structures must be dictated by the position of the sulfur atoms within the ligands. In fact, since the non-coordinated sulfur atoms are *trans* to each other in the mbt moieties, the repulsion between them is reduced with a smaller N–Ru–S angle, getting a more stabilized structure for the $[Ru(dppb)(mbt)_2]$ complex. The same can be suggested for the coordinated sulfur atoms. Here, again, the *trans* position should probably occur for minimize the electronic density repulsion between the four sulfur atoms in both the complexes. For the $[Ru(dppb)(dmbts)_2]$ complex, the unusually small S(21)–Ru–S(22) angle (71.54(4)°) comparatively to other ruthenium phosphine compounds with mercapto ligands [25], strongly reinforces the conclusion about the repulsion between the coordinated and non-coordinated sulfur atoms of a given ligand.

All Ru–ligand distances obtained for $[Ru(dppb)(mbt)_2]$ and $[Ru(dppb)(dmbts)_2]$ complexes are comparable with those found in other ruthenium phosphine compounds with ligands containing sulfur and/or nitrogen atoms [25–28]. Surprisingly, the Ru–P bond distances are similar in both the $[Ru(dppb)(mbt)_2]$ (2.2697(15) and 2.2733(14) Å) and $[Ru(dppb)(dmbts)_2]$ (2.2837(13) and 2.2959(12) Å) complexes. This observation enables us to suggest that the *trans* influence of the nitrogen and sulfur atoms are practically identical. These results, however, can be better analyzed if considering two distinct effects: (i) the higher *trans* influence of the sulfur atom comparatively to the nitrogen atom that implies in the Ru–P bonds weakening for the $[Ru(dppb)(dmbts)_2]$ complex and (ii) the competitive effect between the nitrogen and phosphorus atoms (both good π acceptors) which makes the Ru–P bond distances longer than should be expected for the $[Ru(dppb)(mbt)_2]$ compound. Coincidently, these two effects induce indeed equivalent Ru–P distances in both the complexes that are being studied.

For the $[Ru(dppb)(mbt)_2]$ complex, both the Ru–N and Ru–P bonds (Table 2) are slightly smaller comparatively to similar pyridinic ruthenium complexes [29] (Ru–P: 2.3445(6) and 2.3427(6) Å; Ru–N: 2.151(2) and 2.1538(19) Å). This observation may reflect a higher energy level similarity between the Ru dπ orbitals and those of the appropriated symmetry of the mbt ligand, which imply in a more effective π-back-bonding interaction [30]. A comparative analysis among the covalent radii of the nitrogen and phosphorus atoms shows that the former is only 0.36 Å smaller than the latter [31]. Upon coordination, however, the difference between the lengths of the Ru–N and Ru–P bonds is only about 0.12 Å (see Table 2 for the $[Ru(dppb)(mbt)_2]$ complex). This observation hints that the bond strength between the ruthenium and these atoms are very strong and that the nitrogen is indeed as good π acceptor as the phosphorus atom is. The Ru π-back-bonding interaction should be reflected in the electrochemical properties of both compounds in the sense that the nitrogen atom is better π acceptor than the sulfur species, which is better σ donor.

Additionally, the X-ray structural characterizations of the $[Ru(dppb)(mbt)_2]$ and $[Ru(dppb)(dmbts)_2]$ complexes present a diethyl ether ($CH_3CH_2OCH_2CH_3$) and a dichloromethane (CH_2Cl_2) unit inserted in the respective structures. The presence of these species in the structures of $[Ru(dppb)(mbt)_2]$ and $[Ru(dppb)(dmbts)_2]$ complexes must be assigned to the crystallization and synthetic procedure, respectively.

3.2. NMR

The ^{13}C and ^{1}H NMR chemical shifts in $CDCl_3$ obtained for the $[Ru(dppb)(mbt)_2]$ complex are displayed in Table 3, in addition with coupling data, when it were observed. The assignments proposed were based on two-dimension COSY ^{1}H–^{1}H and HMQC ^{1}H–^{13}C spectra and in comparative form with the ^{1}H and ^{13}C spectra acquired for the free ligand in the same experimental conditions.

The ^{1}H and ^{13}C NMR spectra of the $[Ru(dppb)(mbt)_2]$ complex in $CDCl_3$ solution present high-resolution suggesting that the complex may be diamagnetic, i.e., the ruthenium atom is in its reduced state, Ru^{II}. These spectra present, respectively, four ($\delta = 7.17$, 6.86–6.89, 6.91–6.94 and 7.24–7.26 ppm) and seven signals ($\delta = 118.3$, 120.7, 128.5, 129.2, 132.5, 150.8 and 181.9 ppm) ascribed to the mbts ligand after coordination. By accounting for a higher expected C–P coupling constant values for the carbons located on the neighborhood of the P atoms, the signals observed at 31.9, 139.3 and 138 ppm in the ^{13}C NMR spectrum are assigned, respectively, to the CH_2 (Chart 1, a and d), and C1 and C1′ (Chart 1, ring A and B) as described in

Table 3
^{1}H and ^{13}C chemical shifts in $CDCl_3$ for the $[Ru(dppb)(mbt)_2]$ complex

Groups	^{1}H	^{13}C
CH_2a and CH_2d	1.74 d	31.9 t $^{1}J_{^{13}C^{31}P} = 28.8$
CH_2b and CH_2c	2.75 d	24.4 d $^{2}J_{^{13}C^{31}P} = 3.3$
Ring A		
1,1′		139.3 t $^{1}J_{^{13}C^{31}P} = 38.8$
2,2′, 6,6′	7.87–7.88 d 4H	132.9 t $^{2}J_{^{13}C^{31}P} = 8.8$
3,3′, 5,5′	7.17 m 4H	128.0 t $^{3}J_{^{13}C^{31}P} = 8.8$
4,4′	7.07–7.10 t 2H	125.4
Ring B		
1,1′		138.0 t $^{1}J_{^{13}C^{31}P} = 38.8$
2,2′, 6,6′	7.66 d 4H	132.2 t $^{2}J_{^{13}C^{31}P} = 8.8$
3,3′, 5,5′	7.17 m 4H	127.5 t $^{3}J_{^{13}C^{31}P} = 8.8$
4,4′	6.99–7.02 t 2H	122.4
mbts coordinated		
2,2′		181.9
4,4′	7.17 m 2H	128.5
4a,4a′		150.8
5,5′	6.86–6.89 t 2H	118.3
6,6′	6.91–6.94 t 2H	120.7
7,7′	7.24–7.26 d 2H	129.2
7a,7a′		132.5

Table 3. All these signals are observed in a slightly higher field when the mbts species is free of coordination. This downshift observed after interaction with the metal center points for the electronic delocalization capability of the mbts molecule. However, the signal assigned to the 2 and 2′ carbons of the mbts species (Chart 1) presents an unexpected more pronounced high shift from 168.3 ppm when it is free of interaction to 181.9 ppm upon coordination to the *mer*-[$RuCl_3$(dppb)(OH_2)] metallic complex. This shift might be explained if considering a strong deshielding of these atoms, which may happen as a consequence of an withdraw effect. The sulfur or nitrogen atoms that are close to the 2 and 2′ carbons of the mbts species, at once, can induce this effect. Nevertheless, this strong shift is most probably to occur as the consequence of a bond character change in the neighborhood of the 2 and 2′ carbons. In fact, the structure determined by X-ray diffraction (Fig. 1A) points for the formation of a chelate complex as resultant of the mbts S–S bond broken which meaningfully affects the bond character in the vicinity of these atoms.

The $^{31}P\{^1H\}$ spectrum of the [Ru(dppb)($mbt)_2$] complex showed only a single signal, as expected for a symmetrical arrangement of the two phosphorous atoms [27,32]. The observation of this signal at 52 ppm suggests a strong σ donor character for the mbt ligand based on the data reported by MacFarlane et al. [33].

All the resonance data taken together point for the reduced state of the ruthenium metal center in the [Ru(dppb)($mbt)_2$] isolated compound. Aiming to validate the ruthenium oxidation state in this case, the synthesis was performed by using the [$RuCl_2$(dppb)(PPh_3)] complex instead of the *mer*-[$RuCl_3$(dppb)(OH_2)] compound as starting material. The $^{31}P\{^1H\}$ spectrum of the product thus isolated presents, also, a single signal at 52 ppm. This result confidently confirms that the ruthenium atom is in its reduced state, Ru^{II}, in the [Ru(dppb)($mbt)_2$] complex.

3.3. Vibrational analysis

The assignments of the signals observed in the Raman and infrared (IR) vibrational spectra of the [Ru(dppb)-($mbt)_2$] complex were made in a qualitative form by comparison with similar data reported in the literature [34–37] for related compounds and with the signals observed in the vibrational spectra of the mbts and *mer*-[$RuCl_3$(dppb)(OH_2)] start materials.

Apart from the vibrations at 505, 670, 695, 702 and 744 cm^{-1} due to the Ru(PPh_3)$_2$ moiety [36,37], strong signals observed from 400 to 750 cm^{-1} in the IR and Raman vibrational spectra of the [Ru(dppb)($mbt)_2$] complex are assigned to the C–S stretch frequencies, *ν*(C–S) [34]. The absence of the signal at 536 cm^{-1}, assigned to the S–S stretch frequency *ν*(S–S) [38], in the Raman spectrum of the [Ru(dppb)($mbt)_2$] complex compared with the spectrum of the mbts ligand free of coordination, indicates that the S–S bridge was really broken upon coordination.

The ring breathing is observed as a strong signal at 1008 cm^{-1} in the IR spectrum of the mbts ligand, as expected for aromatic species [34,35]. In the [Ru(dppb)($mbt)_2$] spectrum, however, it appears around 996 cm^{-1}. This downshift may be supported by the high aromaticity of the ring due the delocalization of the bonding electrons around the conjugated ring system [39]. According to Taube [40], an enhancement in the electronic density of a molecule that is coordinated to a given metal center may occur if the metal is in its own reduced state and if the ligand considered holds an appropriated set of LUMO orbitals that enable it to act as a π acid. As pointed out by the X-ray and NMR results, the ruthenium metal center is very probably in the 2+ state and, in such case, one must expect for its π-back-bonding interaction capability with the π appropriated mbt orbitals. In fact, the N-heterocyclic class of ligands is currently cited by the literature [41,42] as presenting a good π acceptor character that facilitates the π-back-bonding interaction of metals such as Fe, Ru and Os.

The bands observed from 1610 to 1660 cm^{-1} are tentatively assigned to the C=C coupled with C=N stretch modes *ν*(C=C + C=N). For some similar compounds, the literature points for a *ν*(C=C + C=N) frequency downshift also based on aromaticity degree increment [39]. With this consideration in mind, the observation of the shift from 1660 cm^{-1} in the IR of the mbts to 1651 cm^{-1} in the IR spectrum of the [Ru(dppb)($mbt)_2$] complex is indicative of an enhancement of the electronic density on the ligand as a consequence of the π-back-bonding effect of the ruthenium metal center.

3.4. Electronic analysis

The electronic spectrum of the [Ru(dppb)($mbt)_2$] complex in CH_2Cl_2 solution presents three bands at 240 ($\varepsilon = 1.59 \times 10^4\ M^{-1}\ cm^{-1}$), 350 ($\varepsilon = 1.59 \times 10^4\ M^{-1}\ cm^{-1}$) and 685 nm ($\varepsilon = 262\ M^{-1}\ cm^{-1}$), besides a shoulder around 276 nm. The two bands and the shoulder observed at higher energies are presented too in the electronic spectrum of the *mer*-[$RuCl_3$(dppb)OH_2] complex in CH_2Cl_2 solution [10,43]. Additionally, the absorption observed at 240 nm must involve the pπ* ← pπ mbt intraligand transitions once the bands at 230 and 273 nm are observed in the electronic spectrum of the mbts ligand free of coordination in CH_2Cl_2 solution.

For the [Ru(dppb)($mbt)_2$] complex, the absorption at 685 nm is assigned to a charge-transfer transition because of its sensitivity toward solvent changes, i.e., in acetonitrile it is observed at 677 nm. Based on the qualitative molecular orbital diagram for compounds of approximately octahedral geometry [44,45], this electronic transition is believed to occur from the ruthenium dπ to the mbt pπ* orbitals, which characterizes a metal-to-ligand charge-transfer transition. Low extinction coefficients for charge-transfer transitions were also observed for a series of $[Ru(NH_3)_5L]^{3+}$ type complexes, where L = dithioether ligands [46]. This

Table 4
UV–Vis (λ and ε) and $Ru^{III/II}$ half-wave formal potential, $E_{1/2}$ (in V vs. NHE), for some ruthenium complexes

Complex	λ_{max}/nm (ε/L mol^{-1} cm^{-1})[a]	$E_{1/2}$[b]	Reference
[Ru(dppb)(dmbts)$_2$]	xx[c]	0.42	this work
[RuCl$_2$(dppb)(4-NH$_2$py)$_2$]	xx[c]	0.45	[27]
[RuCl$_2$(dppb)(4-Nme$_2$py)$_2$]	680 (70)	0.52	[27]
[RuCl$_2$(dppb)(py)$_2$]	672 (90)	0.70	[27]
[RuCl$_2$(dppb)(1,4-dt)]	530 (2000)	0.74	[48]
[Ru(dppb)(mbt)$_2$]	685 (262)	0.78	this work
[RuCl$_2$(dppb)(4-CNpy)$_2$]	675 (105)	0.84	[27]

[a] Solvent: CH_2Cl_2.
[b] All electrochemical data were obtained in CH_2Cl_2 containing 0.1 M TBAP.
[c] Data not available.

result, in accordance with those obtained by NMR and vibrational spectroscopies, strongly suggests that the metal center is in the reduced state, Ru^{II}, in spite of the fact that in the start complex, *mer*-[RuCl$_3$(dppb)(OH$_2$)], the ruthenium was in the oxidized state, Ru^{III}. Bands assigned to the metal-to-ligand charge-transfer transitions in the visible region are also observed for a series of ruthenium(II) phosphine compounds [47].

For correlation purposes, UV–Vis data assigned to the charge-transfer transitions involving the ruthenium metal atom of a set of ruthenium phosphine compounds are set out in Table 4.

All absorbance data but that obtained for the [RuCl$_2$(dppb)(1,4-dt)] complex, are too proximate to reasonably infer any degree difference in the Ru π-back-bonding capability in function of a change of the N-pyridyl ligand. For the [RuCl$_2$(dppb)(1,4-dt)] complex, the observation of the charge-transfer transition in relatively higher energy is explained based on a strong interaction between the dπ orbitals of ruthenium with the d orbitals of sulfur [48,49].

3.5. Electrochemical study

Cyclic voltammetry of the [Ru(dppb)(mbt)$_2$] complex displays a well-defined wave assigned to the $Ru^{III/II}$ redox process. This process is observed with characteristics of high reversibility [50]. The half-wave formal potential value, $E_{1/2} = (E_a + E_c)/2$, where E_a and E_c are the anodic and cathodic potentials, respectively, is observed at 0.78 V. For correlation purpose, this data together with few ones reported in the literature for some relevant ruthenium phosphine complexes are compiled in Table 4.

The $E_{1/2}$ values described in Table 4 enable us to rationalize the order dmbts <4-NH$_2$py < 4-Nme$_2$py < py < 1,4-dt < mbt < 4-CNpy of π electron withdrawing ability in the sense that higher the π back-bonding capability of the metal center, higher will be the $E_{1/2}$ value for its respective redox process, i.e., the metal oxidation is made more difficult to occur. In this way, one might classify the mbt ligand as an excellent acceptor of π electron density. This comment is consistent with the vibrational discussion in which the downshift of some relevant mbt bands after coordination was assigned to the increment of the aromaticity due to the delocalization of the bonding electrons around the ring system [39].

The relatively higher potential (0.74 V) observed for the [RuCl$_2$(dppb)(1,4-dt)] complex (Table 4) in which the sulfur atoms are the unique coordination sites of the ligand is assigned [48] to the strong π back-bonding interaction with the sulfur atoms. This observation hints that the coordination to sulfur atoms comparatively to nitrogen atoms gives raise to a stronger stabilization of the ruthenium metal center in its reduced state. This conclusion is an additional evidence that the coordination of the mbt ligand ought to involve one of its sulfur atoms.

Also, the cyclic voltammogram obtained for the [Ru(dppb)(mbt)$_2$] complex in a more opened potential window (from −1.2 to +1.2 V versus NHE) does not present any additional wave beyond that already commented ($E_{1/2} = 0.78$ V). The cyclic voltammogram of the mbts ligand free of coordination obtained in the same experimental conditions of the [Ru(dppb)(mbt)$_2$] complex, shows two processes. A reduction at −0.72 V, which in turn displays a reoxidation peak at +0.46 V. This reoxidation process is more clearly visualized when the electrode potential is applied in the reverse scan. The wave at −0.72 V is assigned to the reduction of the S–S bridge of the mbts ligand, thus forming the 2-mercaptobenzothiazole (mbt) molecule and that at 0.46 V to the oxidation of the mbt to the mbts. Similar behavior was also observed for the 4,4′-dithiodipyridine (pySSpy) organothiol ligand [51] in an aqueous phosphate buffer solution (pH 7.0). For this species, the potential observed at −0.16 V was assigned to the pySSpy reduction to 4-mercaptopyridine (pyS), and the pyS thus formed was reoxidized to pySSpy at +0.69 V. Accounting for the aprotic medium in which the mbts electrochemical measurements were acquired, the more negative reduction potential (−0.72 V), comparatively to that observed for the pySSpy (−0.16 V), may be explained based on the higher electronic density on the mbts sulfur bridge that makes the S–S bond more robust and so more difficult to be reduced. In reality, it has been shown by the literature that the S–S bond is really affected by the induction of an external electronic density [42,52].

These results reinforce the conclusions obtained from the X-ray and vibrational results concerning the cleavage of the mbts S–S bridge, i.e., if this bond had not be broken, some redox process would be observed around −0.73 V.

3.6. SAMs electroactivity

The electroactivity of the self-assembled monolayers (SAMs) formed on the gold surface by the mbts ligand (mbtsAu) was analyzed by cyclic voltammetry by using the cyt *c* metalloprotein as a probe molecule. The efficiency of this SAM in the assessment of the cyt *c* heterogeneous electron transfer (hET) reaction was compared with that

reported [7,8] for the SAM formed onto gold by the $[Ru(CN)_5(pyS)]^{4-}$ complex (RupySAu). Fig. 2 illustrates the cyclic voltammograms of a cyt *c* solution in physiological medium by using the mbtsAu and RupySAu electrodes.

Although the curve obtained with the RupySAu electrode is clearly better defined than that obtained for the mbtsAu electrode, these cyclic voltammograms point for the efficiency of the SAMs to assess the fast cyt *c* hET reaction. For the mbtsAu electrode, however, the sequence of scans presents a gradual reduction of the current and shape deformation indicating the mbts desorption process. Lamp et al. [53] observed similar behavior for the SAM formed by pyS on gold and used a set of infrared reflection spectra to show that this happens because of a structural conversion on the substrate yielding monolayers composed of atomic and/or oligomeric sulfur species due to the C–S bond cleavage of this molecule. For this experimental reason it was not possible to esteem the cyt *c* hET rate constant, k^0, by using the Nicholson method [54] when the mbtsAu electrode is used. This relatively poor result may be assigned to the conformation of the mbts molecule on the surface as pointed out by the SERS spectrum, which is illustrated in Fig. 3.

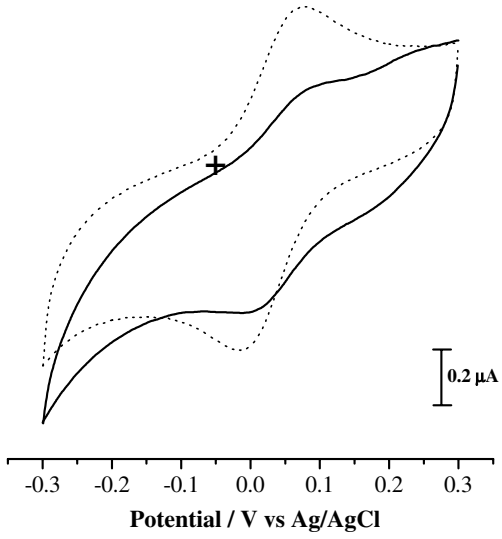

Fig. 2. Cyclic voltammogram at 100 mV s^{-1} of 1 mM cyt *c* in 100 mM KH_2PO_4, pH 7, solution with the mbtsAu (solid line) and RupySAu (dot line) electrodes. + ($i = 0.0$).

Comparatively to the normal Raman spectrum of the mbts species in the solid state (Fig. 3, dot line), the absence of the signal at 536 cm^{-1}, assigned to the ν(S–S) [38], in the SERS spectrum of the mbts SAM (Fig. 3, solid line), indicates the cleavage of the S–S bridge on the gold surface. Similar behavior was observed for the SAM formed by pySSpy on the gold surface [51]. The intensities of the bands in the range from 300 to 800 cm^{-1} observed in the mbts normal Raman due to the out-of-plane vibrational modes of the ligand [36,55,56] are strongly reduced in the mbtsAu surface spectrum. This result suggests that the mbts is chemisorbed on the gold surface in a perpendicular orientation [57] as suggested by the inset in Fig. 3. For this conformation, the adsorbate is expected to bind the gold surface through sulfur σ interaction. In fact, this strong affinity of thiol groups for gold surfaces is well documented in the literature [2].

The gold electrode modified by the $[Ru(dppb)(mbt)_2]$ complex (RumbtAu) electrode has not shown electroactivity toward the electrochemical response of the cyt *c* redox process, even after 72 h of immersion. This observation may be explained based on the groups that are pointing for the solution. Accounting for the coordination through the nitrogen and one of the bridge sulfur atoms of the mbt ligand, the chemisorption on gold through the mbt sulfur atoms, if occurs, make the phosphine moieties as the functional terminal groups, i.e., the ones that will be in contact

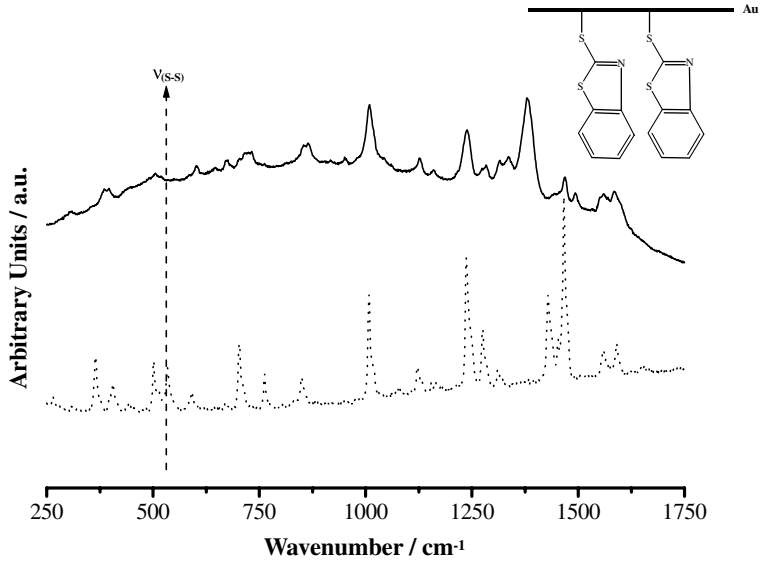

Fig. 3. Normal Raman (dot line) of the mbts ligand in the solid state and SERS spectra (solid line) of the mbts SAM on gold.

with the redox active species in solution. For get an effective molecular recognition with cyt *c* molecules, terminal functional groups that are anionic or weakly basic for interacting with the lysine terminal ends of the cyt *c* that are positively charged in physiological medium, have been claimed by the literature [5,20]. Probably, the phosphine groups do not furnish an optimum geometrical arrangement and/or electronic density for cyt *c* to be recognized. In fact, when species that are not in a normal position in relation to the electrode surface are used for assessment of the cyt *c* hET reaction, this process is weakly or even not observed [58].

4. Conclusions

The structural characterizations (X-ray and NMR) show that the compounds synthesized from the coordination of the mbts and dmbts ligands to the *mer*-[$RuCl_3$(dppb)-(OH_2)] and [$RuCl_2$(dppb)(PPh_3)] complexes, respectively, are chelate species with two four-membered rings. For the [Ru(dppb)($mbt)_2$] complex, the electrochemical, vibrational and electronic data taken together point for the reduced state of the ruthenium metal center, Ru^{II}, despite the 3+ oxidation state of this atom in the *mer*-[$RuCl_3$(dppb)(OH_2)] start complex. This reducing process as well as that of the mbts to mbt molecules are suggested to be due to the methanol interference, which is strongly affected by the *N*-methylmorpholine presence in the reactional medium. The stability enhancement of the ruthenium metal atom in the reduced state in the [Ru(dppb)($mbt)_2$] complex is ascribed to the π-back-bonding interaction between the dπ orbitals of this metal with the π appropriated orbitals of the mbt ligand. Comparatively to other N-heterocyclic ligands, the mbt ligand can be classified as a good π acceptor.

The electroactivity study of the SAM formed by the [Ru(dppb)($mbt)_2$] complex in cyt *c* solution did not present any redox process. This result is assigned to the conformation of the complex on gold surface that does not permit the metalloprotein to be recognized. On the other hand, the SAM formed by the mbts ligand on gold, for which the SERS spectrum shows that the S–S bridge is broken on the surface thus forming a monolayer composed of mbt units, assess the cyt *c* redox process in solution. However, the performance of this SAM should not be comparable with that reported for the RupySAu because of the mbt gradual desorption process.

Appendix A. Supplementary data

Complete tables of bond lengths and angles, final atomic coordinates and equivalent isotropic thermal parameters, calculated hydrogen parameters, anisotropic thermal parameters, and structure factors for the structures are available as supplementary material. Also, tables of atomic coordinates and bond lengths and angle were deposited with the Cambridge Crystallographic Data Center. The respective numbers for the [Ru(dppb)($mbt)_2$] and [Ru(dppb)($dmbts)_2$] complexes are CCDC 251546 and 251547. Supplementary data associated with this article can be found, in the online version, at doi:10.1016/j.ica.2005.05.042.

References

[1] T. Naota, H. Hakaya, S.-I. Murahashi, Chem. Rev. 98 (1998) 2599.
[2] D.M. Kolb, Angew. Chem. Int. Ed. 40 (2001) 1162.
[3] F.A. Armstrong, H.A.O. Hill, N.J. Walton, Acc. Chem. Res. 21 (1988) 407.
[4] F.M. Hawkridge, I. Taniguchi, Comments Inorg. Chem. 17 (1995) 163.
[5] P.M. Allen, H.A.O. Hill, N.J. Walton, J. Electroanal. Chem. 178 (1984) 69.
[6] I.C.N. Diógenes, F.C. Nart, M.L.A. Temperini, I.S. Moreira, Electroanalysis 14 (2002) 153.
[7] I.C.N. Diógenes, F.C. Nart, M.L.A. Temperini, I.S. Moreira, Inorg. Chem. 40 (2001) 4884.
[8] I.C.N. Diógenes, J.R. Sousa, I.M.M. Carvalho, M.L.A. Temperini, A.A. Tanaka, I.S. Moreira, Dalton Trans. 11 (2003) 2231.
[9] Q. Wan, N. Yang, J. Electroanal. Chem. 527 (2002) 131.
[10] L.R. Dinelli, A.A. Batista, K. Wohnrath, M.P. Araujo, S.L. Queiroz, M.R. Bonfadini, G. Oliva, O.R. Nascimento, P.W. Cyr, K.S. MacFarlane, B.R. James, Inorg. Chem. 38 (1999) 5341.
[11] C.E. Jung, P.E. Garrou, P.R. Hoffman, K.G. Caulton, Inorg. Chem. 23 (1984) 726.
[12] P.K. Singh, M.M. Jones, G.R. Gale, L.M. Atkins, R.A. Bulman, J. Toxicol. Environ. Health 28 (1989) 501.
[13] D.L. Brautigan, M.S. Ferguson, E. Margoliash, Methods Enzymol. 53 (1978) 128.
[14] M.D. Hargreaves, M.F. Mahon, M.K. Whittlesey, Inorg. Chem. 41 (2002) 3137.
[15] Enraf-Nonius, COLLECT, Nonius BV, Delft, The Netherlands, 1997–2000.
[16] Z. Otwinowski, W. Minor, HKL Denzo and Scalepack, in: C.W. CarterJr., R.M. Sweet (Eds.), Methods in Enzymology, vol. 276, Academic Press, New York, 1997, p. 307.
[17] R.H. Blessing, Acta. Crystallogr., Sect. A 51 (1995) 33.
[18] G.M. Sheldrick, SHELXS-97: Program for Crystal Structure Resolution, University of Göttingen, Göttingen, Germany, 1997.
[19] L.J. Farrugia, ORTEP3 for Windows, J. Appl. Crystallogr. 30 (1997) 565.
[20] F.A. Armstrong, Struct. Bond. 72 (1990) 137.
[21] P. Gao, D. Gosztola, L.-W.H. Leung, M.J. Weaver, J. Electroanal. Chem. 233 (1987) 211.
[22] X. Qu, T. Lu, S. Dong, J. Mol. Catal. 102 (1995) 111.
[23] D.T. Sawyer, A. Sobkowiak, J.L. Roberts Jr., Electrochemistry for Chemists, second ed., Wiley, New York, 1995.
[24] E.A. Seddon, K.R. Seddon, The Chemistry of Ruthenium, Elsevier, New York, 1984.
[25] P.G. Jessop, C.-L. Lee, G. Rastar, B.R. James, C.J.L. Lock, R. Faggiani, Inorg. Chem. 31 (1992) 4601.
[26] R. Mukherjee, Coord. Chem. Rev. 203 (2000) 151.
[27] S.L. Queiroz, A.A. Batista, G. Oliva, M.T. do, P. Gambardella, R.H.A. Santos, K.S. MacFarlane, S.J. Rettig, B.R. James, Inorg. Chim. Acta 267 (1998) 209.
[28] M.K. Motlagh, N. Safari, C.B. Pamplin, B.O. Patrick, B.R. James, Inorg. Chim. Acta 320 (2001) 184.
[29] J.G. Malecki, J.O. Dzięgielewski, R. Kruszynski, T.J. Bartczak, Inorg. Chem. Commun. 6 (2003) 721.
[30] C.R. Johnson, R.E. Shepherd, Inorg. Chem. 22 (1983) 2439.
[31] J.E. Huheey, E.A. Keiter, R.L. Keiter, Inorganic Chemistry, Principles of Structure and Reactivity, fourth ed., Harper Collins College Publisher, New York, 1993.
[32] A.A. Batista, L.A.C. Cordeiro, G. Oliva, O.R. Nascimento, Inorg. Chim. Acta 258 (1997) 131.

[33] K.S. MacFarlane, A.M. Joshi, S.J. Rettig, B.R. James, Inorg. Chem. 35 (1996) 7304.
[34] C.D. Dyer, J.D. Kilburn, W.F. Maddams, P.A. Walker, Spectrochim. Acta A 47 (1991) 1225.
[35] J.H.S. Green, W. Kynaston, H.M. Paisley, Spectrochim. Acta 19 (1963) 549.
[36] S. Bhattacharya, C.G. Pierpont, Inorg. Chem. 30 (1991) 1511.
[37] P.K. Sinha, L.R. Falvello, S.M. Peng, S. Bhattacharya, Polyhedron 19 (2000) 1673.
[38] F.R. Dollish, W.G. Fateley, F.F. Bentley, Characteristic Raman Frequencies of Organic Compounds, Wiley, New York, 1974.
[39] K.R.G. Devi, D.N. Sathyanarayana, E.M. Engler, J. Mol. Struct. 71 (1981) 1.
[40] H. Taube, in: S.S. Isied (Ed.), Electron Transfer Reactions, vol. 253, Advanced Chemical Series, Washington, DC, 1997, pp. 1–17.
[41] L.M. Baraldo, P. Forlano, A.R. Parise, L.D. Slep, J.A. Olabethe, Coord. Chem. Rev. 219–221 (2001) 881.
[42] I.S. Moreira, J.B. de Lima, D.W. Franco, Coord. Chem. Rev. 196 (2000) 197.
[43] S.-X. Xiao, W.C. Trogler, D.E. Ellis, Z. Berkovitch-Yellin, J. Am. Chem. Soc. 105 (1983) 7033.
[44] P. Ford, D.F.P. Rudd, R. Gaunder, H. Taube, J. Am. Chem. Soc. 90 (1968) 1187.
[45] E. Stuls, J.K.M. Sanders, M. Montalti, L. Prodi, N. Zaccheroni, F.F. Biani, E. Grigiotti, P. Zanello, Inorg. Chem. 41 (2002) 5269.
[46] C.G. Kuehn, S.S. Isied, Prog. Inorg. Chem. 27 (1979) 153.
[47] F. Basuli, S.-M. Peng, S. Bhattacharya, Inorg. Chem. 40 (2001) 1126.
[48] M.O. Santiago, J.R. Sousa, I.C.N. Diógenes, L.G.F. Lopes, E. Meyer, E.E. Castellano, J. Ellena, A.A. Batista, I.S. Moreira, Polyhedron (2005) in press.
[49] C. Stein, H. Taube, Inorg. Chem. 18 (1979) 2212.
[50] A.J. Bard, L.R. Faulkner, Electrochemical Methods: Fundamentals and Applications, Wiley, New York, 1980.
[51] I. Taniguchi, M. Iseki, H. Yamaguchi, K. Yasukouchi, J. Electroanal. Chem. 186 (1985) 299.
[52] I.S. Moreira, D.W. Franco, Inorg. Chem. 33 (1994) 1607.
[53] B.D. Lamp, D. Hobara, M.D. Porter, K. Nili, T.M. Cotton, Langmuir 13 (1997) 736.
[54] R.S. Nicholson, Anal. Chem. 37 (1965) 1351.
[55] D. Cook, Can. J. Chem. 39 (1961) 2009.
[56] E. Spinner, J. Chem. Soc. (1960) 1237.
[57] T. Sawaguchi, F. Mizutani, I. Taniguchi, Langmuir 14 (1998) 3565.
[58] S. Larsson, J. Chem. Soc., Faraday Trans. 79 (1983) 1375.